
[View Journal Online](#)
[View Article Online](#)

Synthesis, crystal structure, Hirshfeld surface analysis, and DFT studies on (2,2'-bipyridine)chlorobis(*N,N*-bis(thiophen-2-ylmethyl)dithiocarbamato-*S,S'*)zinc(II) complex

 Soundararajan Eswari  and Subbiah Thirumaran *

Department of Chemistry, Faculty of Science, Annamalai University, Annamalainagar 608 002, India

 * Corresponding author at: Department of Chemistry, Faculty of Science, Annamalai University, Annamalainagar 608 002, India.
 e-mail: sthirumaran@yahoo.com (S. Thirumaran).

RESEARCH ARTICLE



doi 10.5155/eurjchem.13.1.91-98.2212

 Received: 15 November 2021
 Received in revised form: 20 December 2021
 Accepted: 26 December 2021
 Published online: 31 March 2022
 Printed: 31 March 2022

KEYWORDS

 Ligand
 IR spectroscopy
 Crystal structure
 Zinc(II) dithiocarbamate
 Density functional theory
 Hirshfeld surface analysis

ABSTRACT

Bis(N,N-bis(thiophen-2-ylmethyl)dithiocarbamato-*S,S'*)zinc(II) complex (1) and (2,2'-bipyridine)chlorobis(*N,N*-bis(thiophen-2-ylmethyl)dithiocarbamato-*S,S'*)zinc(II) complex (2) were synthesized. Complex 2 (final product) was structurally characterized by single crystal X-ray diffraction studies. Complex 2 (C₂₁H₁₈ClN₃S₄Zn) crystallized in triclinic crystal system with space group *P*-1 (no. 2), *a* = 8.7603(4) Å, *b* = 10.7488(6) Å, *c* = 13.0262(7) Å, α = 103.965(2)°, β = 91.913(2)°, γ = 104.944(2)°, *V* = 1144.07(10) Å³, *Z* = 2, *T* = 302(2) K, μ (MoK α) = 1.569 mm⁻¹, *D*_{calc} = 1.572 g/cm³, 14892 reflections measured (4.838° ≤ 2 θ ≤ 56.52°), 5570 unique (*R*_{int} = 0.0188, *R*_{sigma} = 0.0230) which were used in all calculations. The final *R*₁ was 0.0810 (*I* > 2 σ (*I*)) and *wR*₂ was 0.2788 (all data). Complex 2 displays distorted square pyramidal coordination geometry. Crystal structure analysis of complex 2 shows that the crystal packing is mainly stabilized by C-H... π (chelate) and C-H...Cl interactions. Hirshfeld surface analysis was carried out to explore deeply into the nature and type of non-covalent interactions. The molecular and electronic structures of complexes 1 and 2 were also studied by DFT quantum chemical calculations.

 Cite this: *Eur. J. Chem.* 2022, 13(1), 91-98

 Journal website: www.eurjchem.com

1. Introduction

Nowadays, a wide range of chemistry explored and developed around the dithiocarbamates and their metal complexes draws attraction due to their unique chemistry and numerous applications [1-3]. The structural chemistry of group 12 dithiocarbamates has attracted the attention of structural chemistry for past two decades due to their diversity structure and supramolecular association in solid state. There are several structural motifs such as monomeric, dimeric, trimeric, linear chain, and layer motifs that have been reported for group 12 dithiocarbamate complexes [4-6]. Systematic studies indicated that the structures of group 12 dithiocarbamates are influenced by N-bound organic moiety [7,8], the solvent used for crystallization [9], and crystallization time [10]. However, the common structural motif adopted by zinc(II) dithiocarbamates is the one that features chelating ligands and two tridentate ligands leading to a centrosymmetric dimer. Addition of imine ligands (such as pyridine, 2,2'-bipyridine, or 1,10-phenanthroline) to zinc(II) dithiocarbamates, the dimeric motifs are disrupted, resulting in the formation of monomeric imine adducts of zinc(II) dithiocarbamates [11,12]. Due to these interesting structural variations and applications, in this paper,

we report synthesis and DFT studies on complexes *bis(N,N*-bis(thiophen-2-ylmethyl)dithiocarbamato-*S, S'*)zinc(II) complex (1) and (2,2'-bipyridine)chlorobis(*N,N*-bis(thiophen-2-ylmethyl)dithiocarbamato-*S,S'*)zinc(II) complex (2). In addition, the crystal structure and Hirshfeld surface analysis of complex 2 are also presented.

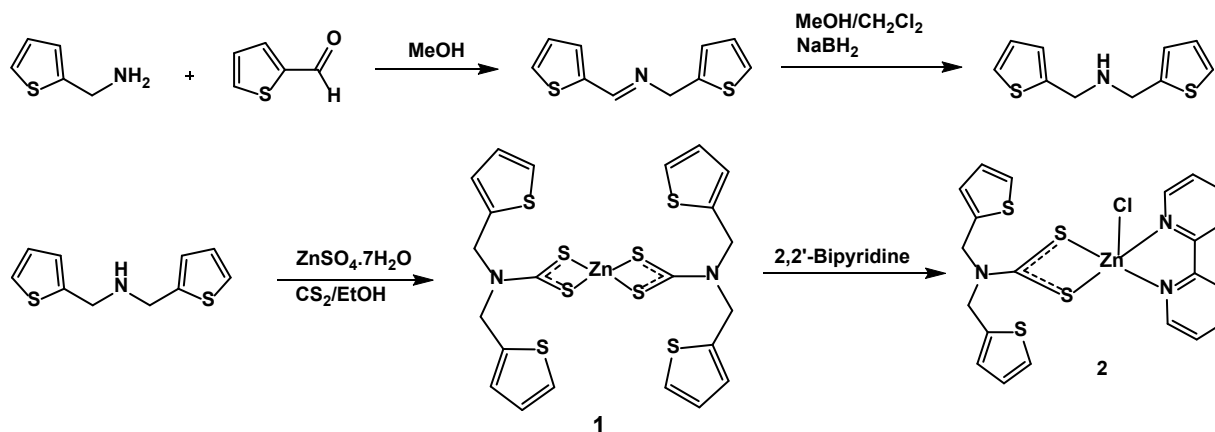
2. Experimental

2.1. Material and methods

2-Thiophenemethylamine and 2-thiophenemethylaldehyde were purchased from Sigma-Aldrich. Zinc sulphate and 2,2'-bipyridine were obtained from Qualigens and SD Fine Chemicals, respectively. All other reagents and solvents were purchased from commercial sources and were used without further purification. FT-IR spectra were recorded in an Agilent-Cary 650 infrared spectrometer in the frequency range 4000-600 cm⁻¹. Single crystal X-ray diffraction measurements of complex 2 were performed using a Bruker D8 QUEST APEX (III) diffractometer (MoK α , λ = 0.71073 Å, Graphite monochromator).

Table 1. Crystal data and structure refinement for complex **2**.

Empirical formula	C ₂₁ H ₁₈ ClN ₃ S ₄ Zn
Formula weight	541.44
Temperature (K)	302(2)
Crystal system	Triclinic
Space group	<i>P</i> -1
<i>a</i> , (Å)	8.7603(4)
<i>b</i> , (Å)	10.7488(6)
<i>c</i> , (Å)	13.0262(7)
α (°)	103.965(2)
β (°)	91.913(2)
γ (°)	104.944(2)
Volume (Å ³)	1144.07(10)
<i>Z</i>	2
ρ _{calc} (g/cm ³)	1.572
μ (mm ⁻¹)	1.569
F(000)	552.0
Crystal size (mm ³)	0.33 × 0.27 × 0.25
Radiation	MoKα (λ = 0.71073)
2θ range for data collection (°)	4.838 to 56.52
Index ranges	-11 ≤ <i>h</i> ≤ 11, -13 ≤ <i>k</i> ≤ 14, -17 ≤ <i>l</i> ≤ 17
Reflections collected	14892
Independent reflections	5570 [R _{int} = 0.0188, R _{sigma} = 0.0230]
Data/restraints/parameters	5570/0/271
Goodness-of-fit on F ²	1.083
Final R indexes [I ≥ 2σ (I)]	R ₁ = 0.0810, wR ₂ = 0.2681
Final R indexes [all data]	R ₁ = 0.0891, wR ₂ = 0.2788
Largest diff. peak/hole (e.Å ⁻³)	2.32/-1.31

**Scheme 1.** Preparation of complexes **1** and **2**.

Using Olex2 [13], the structure was solved by direct methods using the SHELXT 2014/5 [14] program and refined by full-matrix least square on F^2 with SHELXL 2018/3 [15], assuming anisotropic displacement parameters for non-hydrogen atoms. All hydrogen atoms were fixed geometrically. Experimental features related to the X-ray analysis of complex **2** are given in Table 1.

2.2. Theoretical studies

All DFT calculations were carried out for complex **1** and **2** using Gaussian 03 [16]. The molecular structures of complexes **1** and **2** in the ground state were optimized by using DFT method using B3LYP hybrid functional [17] combined with LANL2DZ basis set. The Hirshfeld surface analysis has also been carried out for complex **2** using CrystalExplorer 3.1 program [18,19].

2.3. Synthesis of complexes

Bis(thiophen-2-ylmethyl)amine was prepared using the method reported in the literature [20,21]. Bis(thiophen-2-ylmethyl)amine was prepared by 30 mL of methanol solution containing 2-thiophenemethylamine (0.5 mL, 4.6 mmol) and

thiophene-2-carboxaldehyde (0.5 mL, 5.3 mmol) were stirred at room temperature for 2 h. Then sodium borohydride (499 mg, 13.18 mmol) was added and stirred for 1 h at ice-cold condition. While the reaction mixture was stirred for overnight at room temperature. The secondary amine was separated using dichloromethane (20 mL) solvent.

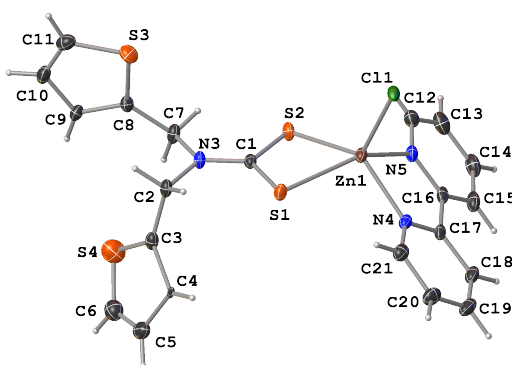
2.3.1. Synthesis of bis(*N,N*-bis(thiophen-2-ylmethyl)dithiocarbamate-*S,S'*)zinc(II) complex (**1**)

Bis(thiophen-2-ylmethyl)amine (0.7 mL, 4.0 mmol) was dissolved in 20 mL of ethanol. To this solution, carbon disulfide (0.3 mL, 4.0 mmol) was added dropwise with constant stirring. Yellow dithiocarbamic acid solution was obtained. An aqueous solution of ZnSO₄·7H₂O (575 mg, 2.0 mmol) was added to this solution. The solid product was collected by filtration and dried in a desiccator (Scheme 1).

Bis(*N,N*-bis(thiophen-2-ylmethyl)dithiocarbamate-*S,S'*)zinc(II) complex (**1**): Color: White. Yield: 65%. M.p.: 195-197 °C. FT-IR (KBr, ν, cm⁻¹): 1474 (ν_{C-N}), 975 (ν_{C-S}). Anal. calcd. for C₂₂H₂₀N₂S₈Zn: C, 41.66; H, 3.18; N, 4.42. Found: C, 41.45; H, 3.14; N, 4.38%.

Table 2. Geometric details of hydrogen bonding (\AA , $^\circ$) in complex 2.

Interactions	D–H	H···A	D···A	\angle D–H···A
C2–H2AB···S1 ^a	0.970	2.568	3.029	109.2
C21–H21···S1 ^a	0.930	2.969	3.532(7)	119.5
C7–H7AB···S2 ^a	0.970	2.481	3.002(6)	113.4
C19–H19···S1 ^b	0.930	3.064	3.818(7)	139.4
C6–H6···Cl1 ^c	0.930	2.919	3.83(1)	165.9
C12–H12···Cl1 ^c	0.930	2.938	3.720(7)	142.9
C15–H15···Cl1 ^c	0.930	2.950	3.590	127.2
C20–H20···Cl1 ^c	0.930	2.913	3.771(9)	154.0
C26–H26··· π (C3, C4, C5, C6, S4) ^d	0.969	2.778	3.473	129.25
C26–H26··· π (Zn1, S1, S2, C1) ^e	0.930	2.992	3.626	126.71

^a Intramolecular C–H···S interaction.^b Intermolecular C–H···S interaction.^c Intermolecular C–H···Cl interaction.^d C–H··· π interactions (pyrrole ring).^e C–H··· π (chelate) interaction.**Figure 1.** Molecular structure of complex 2.

2.3.2. Synthesis of (2,2'-bipyridine)chlorobis(*N,N*-bis(thiophen-2-ylmethyl)dithiocarbamate-*S,S'*)zinc(II) complex (2)

Complex 1 (634 mg, 1 mmol) and 2,2'-bipyridine (312 mg, 2 mmol) were dissolved in hot chloroform (30 mL) and ethanol (10 mL), respectively. The latter hot solution was added dropwise in to the hot chloroform solution. To the resulting yellow solution, petroleum ether (100 mL) was added. The yellow precipitate obtained was filtered and washed with ethanol and dried in a desiccator. The product was recrystallized from chloroform:acetonitrile (3:1, v:v) solution. The chloride ion present in the product presumably arises from chloride extraction from the chloroform. Similar chloride extraction from solvent was observed in the reaction of $\text{Hg}(\text{S}_2\text{CNET}_2)_2$ and 4,7-Me₂-Phen in chloroform to form $[\text{Hg}(\text{S}_2\text{CNET}_2)\text{Cl} (4,7\text{-Me}_2\text{-Phen})]$ [22] (Scheme 1).

(2, 2'-Bipyridine)chlorobis(*N,N*-bis(thiophen-2-ylmethyl)dithiocarbamate-*S,S'*)zinc(II) complex (2): Color: Yellow. Yield: 52%. M.p.: 200–202 °C. FT-IR (KBr, v, cm⁻¹): 1437 ($\nu_{\text{C-N}}$), 966 ($\nu_{\text{C-S}}$). Anal. calcd. for C₂₁H₁₈ClN₃S₄Zn: C, 46.58; H, 3.35; N, 7.76. Found: C, 46.38; H, 3.28; N, 7.68%.

3. Results and discussion

3.1. IR spectral studies

IR spectra of metal dithiocarbamate complexes displayed two characteristic strong bands due to $\nu_{\text{C-N}}$ (thioureide) and $\nu_{\text{C-S}}$ stretching vibrations. In the present study, IR spectra of complexes 1 and 2 show $\nu_{\text{C-N}}$ (thioureide) frequencies at 1474 and 1437 cm⁻¹, respectively, which indicates that C–N bond is intermediate between single and double bond [23]. The $\nu_{\text{C-S}}$ vibrational band was observed as a single band at 975 and 966 cm⁻¹ in the spectra of complexes 1 and 2, respectively, indicating a bidentate coordination of the ligand to the metal center [24].

3.2. Structural analysis of complex 2

Zinc atom in complex 2 has a distorted square pyramidal geometry, being asymmetrically chelated by one *N,N*-bis(thiophen-2-ylmethyl)dithiocarbamate ligand and symmetrically chelated by one 2,2'-bipyridine ligand in the equatorial plane while the fifth coordination site in an axial position is occupied by a chloride ion (Figure 1). The chelate rings defined by Zn1, S1, S2, C1 and Zn1, N4, N5, C16, C17 atoms show a small bite angle deviating 17.84 and 13.4°, respectively, from the ideal angle 90°. As a result, the trans angles (N4–Zn1–S2=135.62(12)° and N5–Zn1–S1=149.10°) subtended, thus significantly deviating from the ideal trans angle of 180°. In the present structure, τ computes to 0.22 which is nearer to an ideal square pyramidal geometry ($\tau = 0$) than to one ideal trigonal bipyramidal with $\tau = 1.0$. The presence of acute ligand bite angles (S1–Zn–S2 = 72.16(4)° and N4–Zn1–N5 = 76.58(18)°) is partially responsible for the observed distortion. The C1–S1 (1.713(5) Å) and C1–S2 (1.725 (5) Å) bond lengths are intermediate between a single and double bond length, thus exhibiting the delocalization of electron density over the NCS₂ unit [25].

The most prominent feature of the molecular packing is the formation of linear chain. The association between molecules is of the type π (chelate) ring···H, whereby the chelate centroid (Zn1, S1, S2, C1)–H19 separation is 2.992 Å (Figure 2a and Table 2). Such C–H··· π (chelate) interactions are well documented [26] in the literature for metal-dithiocarbamate complexes. Crystal structure is further stabilized by intermolecular non-covalent interactions of the C–H··· π (thiophene ring) nature. The adjacent molecules are linked together with numerous weak C–H···Cl intramolecular interactions generating a three-dimensional network (Figure 2b).

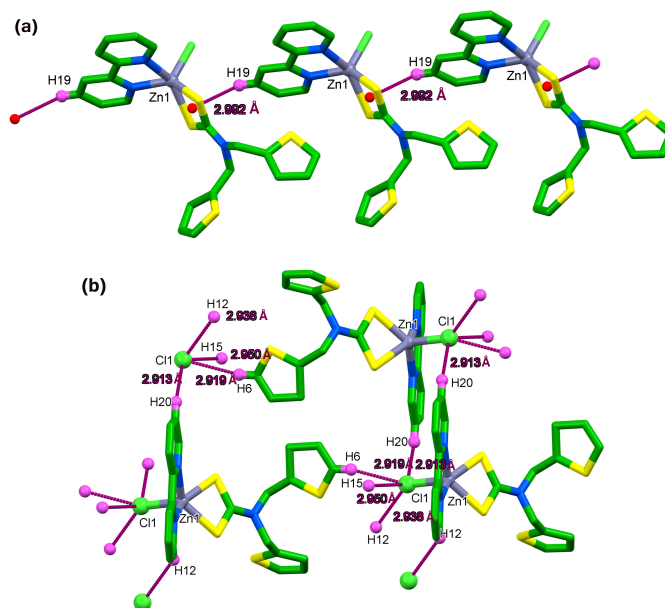


Figure 2. (a) Intermolecular C-H... π (chelate) interaction and (b) Intermolecular C-H...Cl interaction in complex 2.

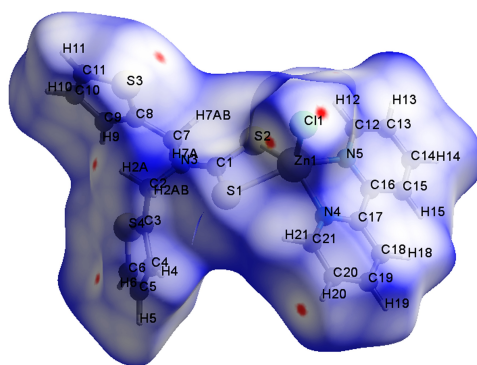


Figure 3. The d_{norm} values were mapped with a white-blue-red colors scheme using Hirshfeld surface of complex 2.

3.3. Hirshfeld surface analysis

The supramolecular interactions in complex **2** were further investigated and visualized by Hirshfeld surface analysis [27]. Figure 3 shows the Hirshfeld surface of complex **2** mapped over d_{norm} . The deep-red circular depressions represent intermolecular short S...H and Cl...H contacts. The finger plots complement the Hirshfeld surface, quantitatively summarizing the nature and type of the intermolecular contacts by describing atom (inside)/atom (outside) interactions (Figure 4). The most significant contributions to the Hirshfeld surface are from H...H (36.5%), C...H/H...C (20.6%), S...H/H...S (15.6%) and Cl...H/H...Cl (12.8%) contacts. These interactions play a crucial role in the overall stabilization of the crystal packing. Other contacts (e.g. S...C/C...S, C...C, N...H/H...N, S...N/N...S, S...S, N...C/C...N and Zn...H/H...Zn) make contribution of less than 4.5% to the Hirshfeld surface [28].

3.4. Optimized geometry

Geometries of complexes **1** and **2** have been fully optimized and are shown in Figure 5. Selected structural parameters are listed in Table 3. The calculated structural parameters for complex **1** are well in consistent with the corresponding values reported for similar monomeric zinc(II) dithiocarbamate complexes [29]. The bond lengths and bond angles of the optimized geometry of complex **2** are compared with those

determined using X-ray diffraction (Table 3). The correlation graphs between the calculated and experimental parameters of bond length and bond angles of complex **2** are calculated as $R^2 = 0.98$ and 0.99 for bond lengths and bond angles, respectively, which indicate the good agreement between the calculated and experimental bond parameters.

3.5. Molecular electrostatic potential (MEP)

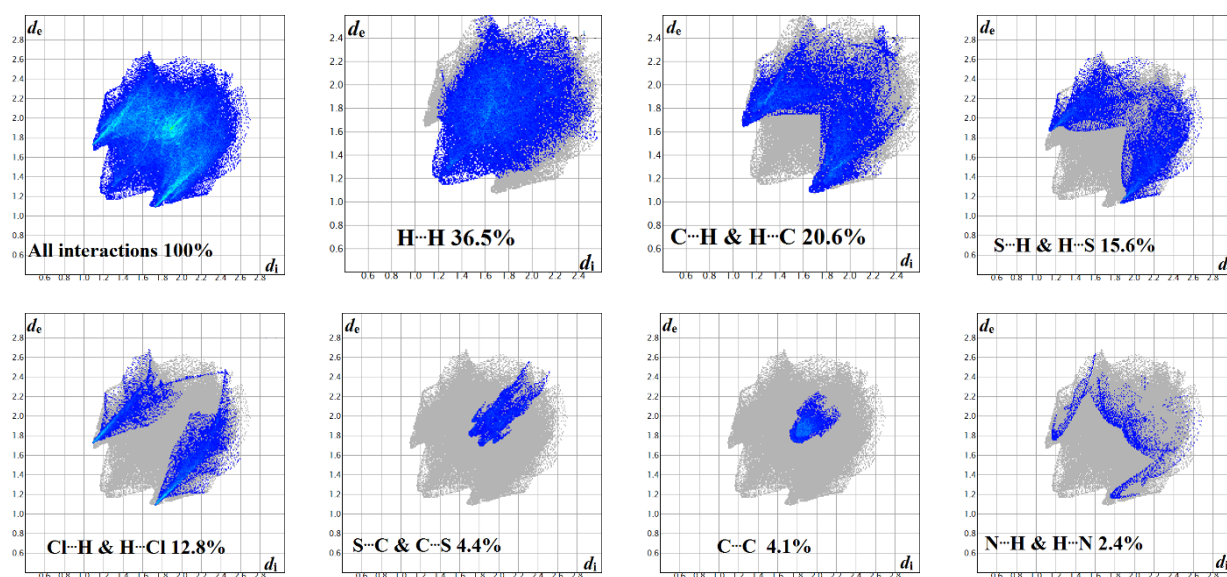
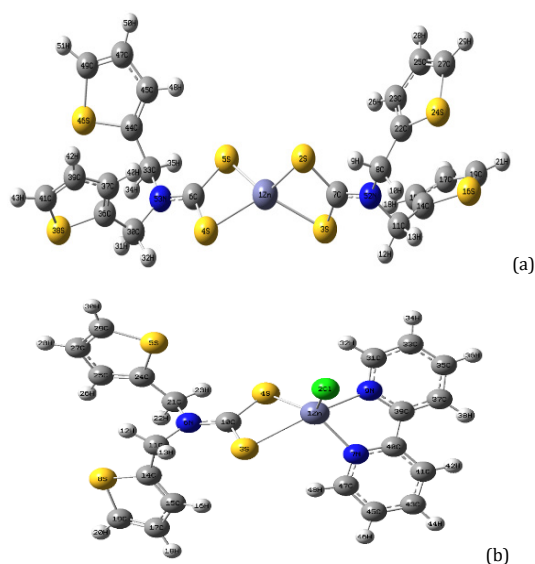
Molecular electrostatic potential of complexes **1** and **2** and the surface maps were developed and are shown in Figure 6. The electric potential diminishes in the following order: red > orange > yellow > green > blue. The electrophilic and nucleophilic sites of a molecule can be distinguished using these different colors [30,31]. In complex **1**, the negative potential regions are located on both sulfur atoms of NCS₂ moiety and the positive regions are located over carbon atoms of NCH₂ groups and hydrogen atoms of thiophene rings. The strongest negative and positive potentials are mainly related to one sulfur atom (orange) and another sulfur atom (blue) of NCS₂, respectively, in complex **2**. All other atoms have slight positive potential (green).

3.6. Frontier molecular orbitals

The frontier molecular orbitals of complexes **1** and **2** are shown in Figure 7.

Table 3. Selected bond length and bond angles in complexes **1** and **2**.

Bond distances (Å) (1)		DFT	Bond distances (Å) (2)		XRD	DFT	Bond angles (°) (2)		XRD	DFT
52N-7C	1.3513		Zn1-N4	2.105(4)	2.105(4)	2.1762	N4-Zn1-N5	76.58(18)	75.47	
7C-2S	1.7994		Zn1-N5	2.161(4)	2.161(4)	2.1997	N4-Zn1-Cl1	107.63(12)	114.86	
7C-3S	1.8004		Zn1-Cl1	2.3053(12)	2.3053(12)	2.3269	N5-Zn1-Cl1	104.45(12)	96.62	
2S-1Zn	2.4913		Zn1-S2	2.3856(15)	2.3856(15)	2.5591	N4-Zn1-S2	135.62(12)	117.58	
3S-1Zn	2.4926		Zn1-S1	2.5917(15)	2.5917(15)	2.6816	N5-Zn1-S2	92.96(12)	92.47	
Bond angles (°) (1)			S1-C1	1.713(5)	1.713(5)	1.7833	Cl1-Zn1-S2	116.74(5)	127.31	
52N-7C-2S	121.23		S2-C1	1.725(5)	1.725(5)	1.7938	N4-Zn1-S1	95.01(13)	95.38	
52N-7C-3S	121.16		N3-C1	1.330(6)	1.330(6)	1.3592	N5-Zn1-S1	149.10(12)	155.72	
2S-7C-3S	117.60					Cl1-Zn1-S1	106.42(5)	108.59		
7C-2S-1Zn	83.03					S2-Zn1-S1	72.16(4)	71.59		
7C-3S-1Zn	82.98					C1-S1-Zn1	82.08(16)	83.23		
2S-1Zn-3S	76.32					C1-S2-Zn1	88.34(17)	86.73		
2S-1Zn-5S	127.86					N3-C1-S1	122.3(4)	121.28		
3S-1Zn-4S	128.29					N3-C1-S2	120.4(4)	120.65		
5S-1Zn-4S	76.38					S1-C1-S2	117.3(3)	118.05		

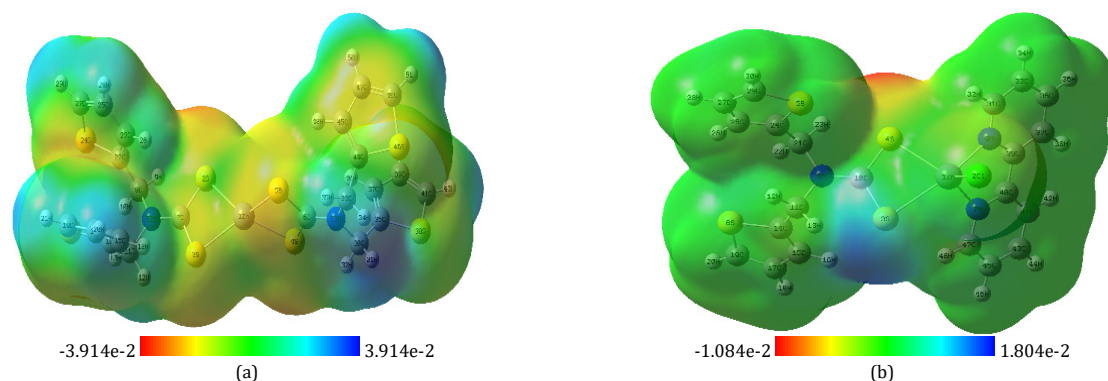
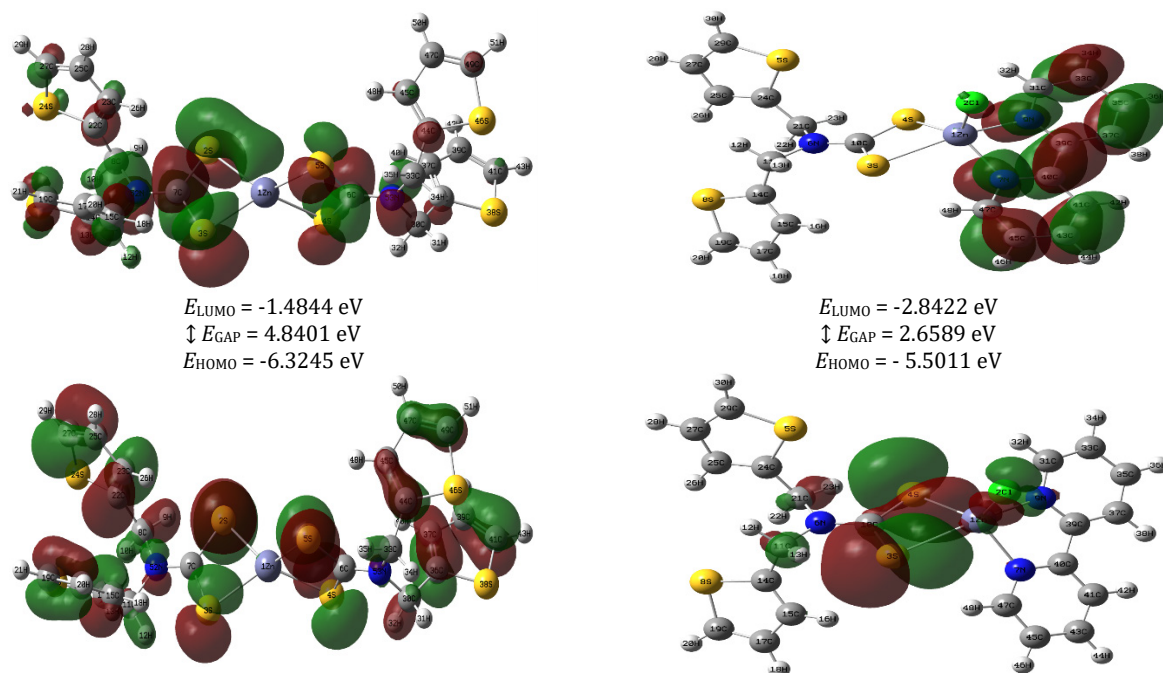
**Figure 4.** The two-dimensional fingerprint plots for complex **2** interactions and delineated into H...H, C...H, S...H, Cl...H, S...C, C...C, and N...H interactions.**Figure 5.** The optimized molecular structure for complexes **1** (a) and **2** (b).

The energy gap between HOMO and LUMO can be used as an indicator of kinetic stability, chemical reactivity, and optical polarizability [32]. In complex **1**, the HOMO is localized in CS₂ moiety, whereas the electronic density of the LUMO is mainly situated in both S atoms of dithiocarbamate ligands. It is

observed that in complex **2**, HOMO is located mainly over both sulfur atoms of NCS₂ and Cl, whereas LUMO is located mainly as 2,2'-bipyridine. The values of the energy gap of complexes **1** and **2** are 4.8401 and 2.6589 eV. These values indicate that complex **1** is more stable than complex **2** and less reactive [24].

Table 4. Global chemical reactivity parameters for complexes **1** and **2**.

Parameter (eV)	Complex 1	Complex 2
Energy (a.u)	-30099.0062	-29829.3962
E_{HOMO}	-6.3245	-5.5011
E_{LUMO}	-1.4844	-2.8422
Energy Gap	4.8401	2.6589
Ionization potential (IP)	6.3245	5.5011
Electron affinity (EA)	1.4844	2.8422
Absolute electronegativity (χ)	3.9045	4.1717
Absolute softness (σ)	0.4132	0.7522
Chemical hardness (η)	2.4201	1.3295
Chemical potential (μ)	-3.9045	-4.1717
Electrophilicity (ω)	3.1458	6.5450

**Figure 6.** MEP map of (a) complexes **1** and (b) **2**.**Figure 7.** Frontier molecular orbitals (FMOs) of (a) complex **1** and (b) complex **2**.

The global reactivity descriptors of complexes **1** and **2** such as absolute electronegativity (χ), softness (σ), hardness (η), chemical potential (μ), and electrophilicity (ω), are obtained using the following equations [32]: $\chi = (I+A)/2$, $\sigma = 1/\eta$, $\eta = (I-A)/2$, $\mu = -\chi$, $\omega = \mu^2/2\eta$ Where $I = -E_{\text{HOMO}}$ and $A = -E_{\text{LUMO}}$ are the ionization potential and electron affinity, respectively. The Global reactivity descriptors values are given in Table 4. Complex **1** showed a higher chemical hardness (2.4201 eV) than that of complex **2** (1.3295 eV). This indicates that complex **1** resist more towards the deformation of the electron density distribution, hence more stable and less reactive compared to

complex **2** [33]. The higher electrophilicity index value of complex **2** indicates that it is the strong electrophile compared to complex **1** [34].

4. Conclusions

Synthesis and characterization of complexes **1** and **2** were presented. Crystal structure of complex **2** showed that zinc(II) is five-coordinated in a distorted square pyramid in complex **2**. The mononuclear (2,2'-bipyridine)chlorobis(*N,N*-bis(thiophen-2-ylmethyl)dithiocarbamato-S,S')zinc(II) complex (**2**) form the

multidimensional frame work by the help of C-H... π (chelate) and C-H...Cl interactions. Hirshfeld surface analysis of complex **2** confirmed the presence of C-H...Cl intermolecular interactions. 2-D finger print plots of complex **2** showed that the major contribution to the total Hirshfeld surface is from H...H (36.5%) contacts. Molecular structures of complexes **1** and **2** were studied using DFT calculations. There is a good agreement between the calculated bond parameters for complex **2** with those derived from the X-ray crystal structure.

Acknowledgements

Support is acknowledged from the donors of the American Chemical Society Petroleum Research Fund (PRF# 12345-AC1); the State of Delaware; the National Institute of General Medical Sciences (P20GM123456) from the National Institutes of Health (INBRE program); and a National Science Foundation (NSF) EPSCoR grant IIA-1234567.

Supporting information

CCDC-2121961 contains the supplementary crystallographic data for this paper. These data can be obtained free of charge via www.ccdc.cam.ac.uk/data_request/cif, or by e-mailing data_request@ccdc.cam.ac.uk, or by contacting The Cambridge Crystallographic Data Centre, 12 Union Road, Cambridge CB2 1EZ, UK; fax: +44(0)1223-336033.

Disclosure statement

Conflict of interest: The authors declare that they have no conflict of interest. Ethical approval: All ethical guidelines have been adhered. Sample availability: Samples of the compounds are available from the author.

CRedit authorship contribution statement

Conceptualization: Subbiah Thirumaran; Methodology: Subbiah Thirumaran; Software: Soundararajan Eswari; Validation: Soundararajan Eswari; Formal Analysis: Soundararajan Eswari; Investigation: Soundararajan Eswari; Subbiah Thirumaran; Resources: Subbiah Thirumaran; Data Curation: Soundararajan Eswari; Writing - Original Draft: Soundararajan Eswari; Writing - Review and Editing: Subbiah Thirumaran; Visualization: Soundararajan Eswari; Supervision: Subbiah Thirumaran;

ORCID and Email

Soundararajan Eswari

 eswariphd1625@gmail.com

 <https://orcid.org/0000-0002-9089-0814>

Subbiah Thirumaran

 sthirumaran@yahoo.com

 <https://orcid.org/0000-0002-5771-5328>

References

- Maurya, V. K.; Singh, A. K.; Singh, R. P.; Yadav, S.; Kumar, K.; Prakash, P.; Prasad, L. B. Synthesis and Evaluation of Zn(II) Dithiocarbamate Complexes as Potential Antibacterial, Antibiofilm, and Antitumor Agents. *J. Coord. Chem.* **2019**, *72* (19–21), 3338–3358.
- Alam, M. N.; Mandal, S. K.; Debnath, S. C. Effect of Zinc Dithiocarbamates and Thiazole-Based Accelerators on the Vulcanization of Natural Rubber. *Rubber Chem. Technol.* **2012**, *85* (1), 120–131.
- Gallagher, W. P.; Vo, A. Dithiocarbamates: Reagents for the Removal of Transition Metals from Organic Reaction Media. *Org. Process Res. Dev.* **2015**, *19* (10), 1369–1373.
- Ajibade, P. A.; Mbese, J. Z.; Omondi, B. Group 12 Dithiocarbamate Complexes: Synthesis, Characterization, and X-Ray Crystal Structures of Zn(II) and Hg(II) Complexes and Their Use as Precursors for Metal Sulfide Nanoparticles. *Inorg. nano-met. chem.* **2017**, *47* (2), 202–212.
- Tiekink, E. Exploring the Topological Landscape Exhibited by Binary Zinc-Triad 1,1-Dithiolates. *Crystals (Basel)* **2018**, *8* (7), 292.
- Singh, V.; Kumar, V.; Gupta, A. N.; Drew, M. G. B.; Singh, N. Effect of Pyridyl Substituents Leading to the Formation of Green Luminescent Mercury(II) Coordination Polymers, Zinc(II) Dimers and a Monomer. *New J Chem* **2014**, *38* (8), 3737.
- Kumar, V.; Manar, K. K.; Gupta, A. N.; Singh, V.; Drew, M. G. B.; Singh, N. Impact of Ferrocenyl and Pyridyl Groups Attached to Dithiocarbamate Moieties on Crystal Structures and Luminescent Characteristics of Group 12 Metal Complexes. *J. Organomet. Chem.* **2016**, *820*, 62–69.
- Gurumoorthy, G.; Thirumaran, S.; Ciattini, S. Unusual Octahedral Hg(II) Dithiocarbamate: Synthesis, Spectral and Structural Studies on Hg(II) Complexes with Pyrrole Based Dithiocarbamates and Their Utility for the Preparation of α - and β -HgS. *Polyhedron* **2016**, *118*, 143–153.
- Eswari, S.; Selvaganapathi, P.; Thirumaran, S.; Ciattini, S. Effect of Solvent Used for Crystallization on Structure: Synthesis and Characterization of Bis(N,N-Di(4-Fluorobenzyl)Dithiocarbamate-S,S') M(II) (M = Cd, Hg) and Usage as Precursor for CdS Nanophoto-catalyst. *Polyhedron* **2021**, *206* (115330), 115330.
- Tan, Y. S.; Sudlow, A. L.; Molloy, K. C.; Morishima, Y.; Fujisawa, K.; Jackson, W. J.; Henderson, W.; Halim, S. N. B. A.; Ng, S. W.; Tiekink, E. R. T. Supramolecular Isomerism in a Cadmium Bis(N-Hydroxyethyl, N-Isopropylidithiocarbamate) Compound: Physicochemical Characterization of Ball (n = 2) and Chain (n = ∞) Forms of Cd[S2CN(IPr)CH2CH2OH]2-solvent. *Cryst. Growth Des.* **2013**, *13* (7), 3046–3056.
- Onwujiwe, D. C.; Nthwane, Y. B.; Ekennia, A. C.; Hosten, E. Synthesis, Characterization and Antimicrobial Properties of Some Mixed Ligand Complexes of Zn(II) Dithiocarbamate with Different N-Donor Ligands. *Inorganica Chim. Acta* **2016**, *447*, 134–141.
- Selvaganapathi, P.; Thirumaran, S.; Ciattini, S. Structural Variations in Zinc(II) Complexes with N,N-Di(4-Fluorobenzyl)Dithiocarbamate and Imines: New Precursor for Zinc Sulfide Nanoparticles. *Polyhedron* **2018**, *149*, 54–65.
- Dolomanov, O. V.; Bourhis, L. J.; Gildea, R. J.; Howard, J. A. K.; Puschmann, H. OLEX2: A Complete Structure Solution, Refinement and Analysis Program. *J. Appl. Crystallogr.* **2009**, *42* (2), 339–341.
- Sheldrick, G. M. SHELXT - Integrated Space-Group and Crystal-Structure Determination. *Acta Crystallogr. A Found. Adv.* **2015**, *71* (Pt 1), 3–8.
- Sheldrick, G. M. Crystal Structure Refinement with SHELXL. *Acta Crystallogr. C Struct. Chem.* **2015**, *71* (Pt 1), 3–8.
- Frisch, M. J.; Trucks, G. W.; Schlegel, H. B.; Scuseria, G. E.; Robb, M. A.; Cheeseman, J. R.; Montgomery J. A.; Vreven, J. T.; Kudin, K. N.; Burant, J. C.; Millam, J. M.; Iyengar, S. S.; Tomasi, J.; Barone, V.; Mennucci, B.; Cossi, M.; Scalmani, G.; Rega, N.; Petersson, G.A.; Nakatsuji, H.; Hada, M.; Ehara, M.; Toyota, K.; Fukuda, R.; Hasegawa, J.; Ishida, M.; Nakajima, T.; Honda, Y.; Kitao, O.; Nakai, H.; Klene, M.; Li, X.; Knox, J. E.; Hratchian, H. P.; Cross, J. B.; Adamo, C.; Jaramillo, J.; Gomperts, R.; Stratmann, R. E.; Yazyev, O.; Austin, A. J. Cammi, R.; Pomelli, C.; Ochterski, J. W.; Ayala, P. Y.; Morokuma, K.; Voth, G. A.; Salvador, P.; Dannenberg, J. J.; Zakrzewski, V.G.; Dapprich, S.; Daniels, A. D.; Strain, M. C.; Farkas, O.; Malick, D. K.; Rabuck, A. D.; Raghavachari, K.; Foresman, J. B.; Ortiz, J. V.; Cui, Q.; Baboul, A. G.; Clifford, S.; Cioslowski, J.; Stefanov, B. B.; Liu, G.; Liashenko, A.; Piskorz, P.; Komaromi, I. Martin, R. L.; Fox, D. J. Keith, T.; Al-Laham, M. A.; Peng, C. Y.; Nanayakkara, A.; Challacombe, M.; Gill, P. M. W.; Johnson, B.; Chen, W.; Wong, M. W.; Gonzalez C.; Pople, J. A. Gaussian 03, Revision B.04, Gaussian, Inc., Pittsburgh PA, 2003.
- Lee, C.; Yang, W.; Parr, R. G. Development of the Colle-Salvetti Correlation-Energy Formula into a Functional of the Electron Density. *Phys. Rev. B Condens. Matter* **1988**, *37* (2), 785–789.
- Wolf, S. K.; Grimwood, D. J.; McKinnon, J. J.; Turner, M. J.; Jayatilaka, D.; Spackman, M. A. Crystal Explorer Ver. 3.1, University of Western Australia, Perth, Australia, 2013.
- Spackman, M. A.; McKinnon, J. J.; Jayatilaka, D. Electrostatic Potentials Mapped on Hirshfeld Surfaces Provide Direct Insight into Intermolecular Interactions in Crystals. *CrystEngComm* **2008**, *10* (4), 377–388.
- Sathiyaraj, E.; Srinivasan, T.; Thirumaran, S.; Velmurugan, D. Synthesis and Spectroscopic Characterization of Ni(II) Complexes Involving Functionalised Dithiocarbamates and Triphenylphosphine: Anagostic Interaction in [N-Cyclopropyl-N-(4-Fluorobenzyl)Dithiocarbamate-S,S'] (Thiocyanato-N)(Triphenylphosphine)Nickel(II). *J. Mol. Struct.* **2015**, *1102*, 203–209.
- Sattigeri, V. J.; Soni, A.; Singhal, S.; Khan, S.; Pandya, M.; Bhatija, P.; Mathur, T.; Rattan, A.; Khanna, J. M.; Mehta, A. Synthesis and Antimicrobial Activity of Novel Thiazolidinones. *ARKIVOC* **2005**, *2005* (2), 46–59.
- Lai, C. S.; Tiekink, E. R. T. Crystallographic Report: Chloro(N,N-Diethyl dithiocarbamate)(4, 7-Dimethyl-1, 10-Phenanthroline) Mercury(II) Hemi-Chloroform Solvate. *Appl. Organomet. Chem.* **2003**, *17* (2), 141–142.
- Tiekink, E. R. T.; Wardell, J. L.; Wardell, S. M. S. V. Hydrogen-Bonding Interactions in the Crystal Structure of Bis[N-Propyl-N-(2-Hydroxy ethyl)Dithiocarbamate-S,S']Nickel(II): Ni[S2CN(NPr)(CH2CH2OH)]2. *J. Chem. Crystallogr.* **2007**, *37* (7), 439–443.
- Alverdi, V.; Giovagnini, L.; Marzano, C.; Seraglia, R.; Bettio, F.; Sitran, S.; Graziani, R.; Fregona, D. Characterization Studies and Cytotoxicity Assays of Pt(II) and Pd(II) Dithiocarbamate Complexes by Means of FT-IR, NMR Spectroscopy and Mass Spectrometry. *J. Inorg. Biochem.* **2004**, *98* (6), 1117–1128.
- Sathiyaraj, E.; Thirumaran, S.; Selvanayagam, S.; Sridhar, B.; Ciattini, S. C H...Ni and C H... π (Chelate) Interactions in Nickel(II) Complexes

- Involving Functionalized Dithiocarbamates and Triphenylphosphine. *J. Mol. Struct.* **2018**, *1159*, 156–166.
- [26]. Tiekink, E. R. T. The Remarkable Propensity for the Formation of C–H... π (Chelate Ring) Interactions in the Crystals of the First-Row Transition Metal Dithiocarbamates and the Supramolecular Architectures They Sustain. *CrystEngComm* **2020**, *22* (43), 7308–7333.
- [27]. Mangasuli, S. N.; Hosamani, K. M.; Managutti, P. B. Synthesis of Novel Coumarin Derivatives Bearing Dithiocarbamate Moiety: An Approach to Microwave, Molecular Docking, Hirshfeld Surface Analysis, DFT Studies and Potent Anti-Microbial Agents. *J. Mol. Struct.* **2019**, *1195*, 58–72.
- [28]. Mehmood, T.; Bhosale, R. S.; Reddy, J. P. Bis(2-Methylpyridinium) Tetrachloridocuprate(II): Synthesis, Structure and Hirshfeld Surface Analysis. *Acta Crystallogr. E Crystallogr. Commun.* **2021**, *77* (7), 726–729.
- [29]. Lakshmanan, P.; Thirumaran, S.; Ciattini, S. Synthesis, Spectral and Structural Studies on NiS₂PN and NiS₂P₂ Chromophores and Use of Ni(II) Dithiocarbamate to Synthesize Nickel Sulfide and Nickel Oxide for Photodegradation of Dyes. *J. Mol. Struct.* **2020**, *1220* (128704), 128704.
- [30]. Prabhuswamy, A.; Mohammed, Y. H. E.; Al-Ostoot, F. H.; Venkatesh, G. D.; Anandalwar, S. M.; Khanum, S. A.; Krishnappagowda, L. N. Synthesis, Crystal Structure Elucidation, Hirshfeld Surface Analysis, 3D Energy Frameworks and DFT Studies of 2-(4-Fluorophenoxy) Acetic Acid. *Eur. J. Chem.* **2021**, *12* (3), 304–313.
- [31]. Krishnan, K. G.; Thanikachalam, V. Synthesis, Spectral, Crystallographic, and Computational Investigation of a Novel Molecular Hybrid 3-(1-((Benzoyloxy)Imino)Ethyl)-2H-Chromen-2-Ones. *Eur. J. Chem.* **2021**, *12* (2), 133–146.
- [32]. Yu, X.; Wang, N.; He, H.; Wang, L. Theoretical Investigations of the Structures and Electronic Spectra of Zn(II) and Ni(II) Complexes with Cyclohexylamine-N-Dithiocarbamate. *Spectrochim. Acta A Mol. Biomol. Spectrosc.* **2014**, *122*, 283–287.
- [33]. Adole, V. A.; Jagdale, B. S.; Pawar, T. B.; Sawant, A. B. Experimental and Theoretical Exploration on Single Crystal, Structural, and Quantum Chemical Parameters of (E)-7-(Arylidene)-1,2,6, 7-tetrahydro-8 H -indeno[5,4- b]Furan-8-one Derivatives: A Comparative Study. *J. Chin. Chem. Soc.* **2020**, *67* (10), 1763–1777.
- [34]. Domingo, L. R.; Ríos-Gutiérrez, M.; Pérez, P. A. Molecular Electron Density Theory Study of the Participation of Tetrazines in Aza-Diels-Alder Reactions. *RSC Adv.* **2020**, *10* (26), 15394–15405.



Copyright © 2022 by Authors. This work is published and licensed by Atlanta Publishing House LLC, Atlanta, GA, USA. The full terms of this license are available at <http://www.eurjchem.com/index.php/eurjchem/pages/view/terms> and incorporate the Creative Commons Attribution-Non Commercial (CC BY NC) (International, v4.0) License (<http://creativecommons.org/licenses/by-nc/4.0>). By accessing the work, you hereby accept the Terms. This is an open access article distributed under the terms and conditions of the CC BY NC License, which permits unrestricted non-commercial use, distribution, and reproduction in any medium, provided the original work is properly cited without any further permission from Atlanta Publishing House LLC (European Journal of Chemistry). No use, distribution or reproduction is permitted which does not comply with these terms. Permissions for commercial use of this work beyond the scope of the License (<http://www.eurjchem.com/index.php/eurjchem/pages/view/terms>) are administered by Atlanta Publishing House LLC (European Journal of Chemistry).